



Universiteit  
Leiden  
The Netherlands

## **Deciphering the complex paramagnetic NMR spectra of small laccase**

Dasgupta, R.

### **Citation**

Dasgupta, R. (2021, June 15). *Deciphering the complex paramagnetic NMR spectra of small laccase*. Retrieved from <https://hdl.handle.net/1887/3188356>

Version: Publisher's Version

License: [Licence agreement concerning inclusion of doctoral thesis in the Institutional Repository of the University of Leiden](#)

Downloaded from: <https://hdl.handle.net/1887/3188356>

**Note:** To cite this publication please use the final published version (if applicable).

Cover Page



Universiteit Leiden



The handle <https://hdl.handle.net/1887/3188356> holds various files of this Leiden University dissertation.

**Author:** Dasgputa, R.

**Title:** Deciphering the complex paramagnetic NMR spectra of small laccase

**Issue Date:** 2021-06-15

## Chapter 7

---

### General Discussion and Prospects

---

### *Mimics for laccases*

Enzymatic biofuel cells (EBC) promise a future of sustainability without adversely affecting the environment. The stability of the enzymes and challenge of functionalizing them on an electrode has, however, limited their application to small devices.(1–3) One way to overcome this disadvantage is to design and synthesize an artificial catalyst based on the active site of enzymes. In the past decade a slew of artificial catalysts has been reported for the enzyme laccase, which catalyzes oxygen reduction at the cathode half of the EBC. Although these catalysts circumvent the issues of instability and immobilization of the laccase, the efficiency of the oxygen reduction reaction was substantially lower than for laccase.(4) There are two prevailing ideas to improve the efficiency of artificial catalysts, (a) incorporating functional groups mimicking the second shell residues and their associated interactions within the active site of laccase and (b) mimicking the motions of the active site residues associated with the complex oxygen reduction reaction. In relation to the latter idea, this thesis aims to lay the groundwork for understanding active site motions in the enzyme small laccase (SLAC).

### *Motions in enzyme active sites*

Enzymes increase the catalytic rate of reaction by stabilizing the transition state. This is achieved by attaining a conformation that has most favorable interactions with the substrate when in its transition state, requiring sub-Ångström precision of positioning of active site atoms. For a multistep process such as oxygen reduction, each step in the reaction is associated with a transition state. The enzyme must therefore change conformation in order to stabilize these successive transition states. Such conformational change during the catalytic cycle is found in many enzymes, for example, alcohol dehydrogenase, dihydrofolate reductase and cytochrome P450.(5–7) In laccase, once the enzyme is reduced from its resting oxidized (RO) state oxygen reduction occurs via the three intermediate states described in Chapter 1, the fully reduced (FR) state, the peroxide intermediate (PI) state and the native intermediate (NI) state. Conformational changes are imperative during this reaction as the interactions at the active site are likely to be different for the transition states of the conversion of dioxygen to peroxide and of peroxide to two separate oxygen atoms. Also, the transfer of protons through the enzyme and binding of oxygen and egress of water molecules may well involve conformational changes of backbone or sidechains. Large conformational changes may themselves have significant activation barriers, to the extent that required conformational changes may become the rate limiting step of the catalytic cycles.

The main goal of the work described in this thesis was to characterize such motions using NMR spectroscopy and to assign them to specific histidine ligands. Characterizing the motions that enable these conformational changes and

implementing them in the bio-inspired catalyst may improve its efficiency. The small size of the inorganic compounds such as discussed in Chapter 1 do not allow for such complicated motions, but a small protein or peptide mimic of the TNC might approach the native system better.

### *Paramagnetic NMR methodology to study motions*

Although the reaction mechanism of laccase has been characterized in detail using multiple crystal structures and quantum calculations, the information about the motions present at the active site was limited. Two crystal structures showed that the histidine ligands of the active site can have two conformations (Chapters 1 and 2). NMR spectroscopy is suitable to identify such motions and determine the exchange rates. In this thesis a  $\sim 105$  kDa trimeric, two-domain laccase, SLAC, was studied. Due to its large size, line broadening caused by the paramagnetic copper ions and large hyperfine shifts it is not possible to use standard multidimensional NMR experiments to study the active site. Therefore, paramagnetically tailored experiment were used in which the delay between the scans and the magnetization transfer between nuclei is reduced to get optimal signal, given the short spin-spin and spin-lattice relaxation times of the nuclei close to the paramagnetic metal center (Chapter 1). Due to the large hyperfine shifts, the signals from the nuclear spins near the metal center in a paramagnetic protein are dispersed over a large spectral region compared to those for diamagnetic proteins. To excite such a large spectral region, short high-power radiofrequency (RF) pulses are required. In addition, standard homonuclear and heteronuclear decoupling methods are found to be inefficient for such a large spectral region and in the worst case it have a deleterious effect on the spectrum.(8) Excitation of multiple smaller spectral regions with changing offset and high power RF pulses can help to resolve this issue.(9) Recent advances in magic angle spinning (MAS) solid state NMR (ssNMR) have also helped in challenging these problems. The sensitivity and resolution of paramagnetic spectrum were improved by using heteronuclear correlation experiments based on transferred-echo double resonance (TEDOR) and dipolar analog of insensitive nuclei enhancement by polarization transfer (D-INEPT) experiment.(10, 11) In these experiments, the polarization transfer time is based on the dipolar coupling strength between the nuclei, which is in  $\mu\text{s}$  to  $\text{ms}$  time scale, thereby efficiently enhancing paramagnetically broadened signals. In addition, very fast MAS ( $> 20$  kHz) has removed the need for decoupling as under such conditions the contribution of the dipolar coupling on the linewidth is sufficiently narrowed.(12) Development of short high-power adiabatic pulses (SHAP) allowed to efficiently excite large spectral windows, ranging from 400 ppm to  $\sim 1000$  ppm.(13)

### *The RO and NI states*

The TNC comprises of a T3 site and a T2 site. Interestingly, the NMR spectra of SLAC were observed to represent a mix of the RO and NI states (Chapters 2, 3 and 4).<sup>(14)</sup> The SLAC wild type (SLAC-wt) was observed to be predominantly in the RO state, while the T1 site depleted mutant (SLAC-T1D) was mostly in the NI state. Perhaps the reason is that in SLAC-wt the T1 site copper confers some structural restraints on the geometry of the T3 site via the HCH motif so as to render the RO state more stable than the NI state.<sup>(14)</sup> In the SLAC-T1D this restraint is absent and the NI state becomes predominant. Interestingly, the double mutant SLAC-T1D/Q291E is exclusively in the RO state.<sup>(14)</sup> This double mutant is discussed in later. It is also observed that the resonances from the RO state are shifted less (11 to 22 ppm) compared to those of the NI state (22 to 55 ppm). The reason is that in the RO state the paramagnetic and diamagnetic states are in fast exchange and the population of the former depends on the energy gap ( $2J$ , equation 1.5). For a  $2J$  of  $-600\text{ cm}^{-1}$ , the population is about 20% at ambient temperature, so the FCS is significantly smaller than of the NI state, which is a frustrated spin system that is paramagnetic in the ground state.

The strong coupling between all the three copper ions in the NI state <sup>(15)</sup> increases the electronic relaxation rate enabling the observation of all histidine ligands (Chapters 3 and 4). Similarly, in the RO state, strong coupling between the T3 copper ions enables the observation of resonance from its histidine ligands, while the resonances of the T2 site histidine ligands are broadened beyond detection.<sup>(16)</sup> It is noteworthy that the N $\epsilon$ 2, C $\delta$ 2-H $\delta$ 2 and C $\epsilon$ 1-H $\epsilon$ 1 nuclei of the histidine ring are not observed. These atoms are  $< 3.5\text{ \AA}$  and one, two or three bonds from the copper ion and thereby have large electron spin density. This excess electron spin density can lead to the signal broadening beyond detection and very large hyperfine shifts. For a type-1 copper proteins like amicyanin and plastocyanin the resonances of the H $\delta$ 2 and H $\epsilon$ 1 nuclei from the histidine ligand could be determined.<sup>(9, 17)</sup> It might be because most of the spin density is localized on the sulfur of the cysteine ligand. This consequently reduces the spin density on the histidine rings thereby enabling the observation of the nuclei very close to the metal center. Saturation transfer experiment can be used to detect signals that are broadened beyond detection in the  $^1\text{H}$  NMR spectrum.<sup>(9)</sup> A “blind” high-power irradiation of the  $^1\text{H}$  spectral region  $\sim 1000\text{ ppm}$  downfield allowed the detection of the resonances from the H $\beta$ 2/3 of the cysteine ligand with linewidths of 519 and 329 kHz in plastocyanin.<sup>(9)</sup> Such experiments are not possible in laccase due to the absence of self-exchange between the diamagnetic and the paramagnetic forms.

The resonances of N $\delta$ 1 and H $\delta$ 1 nuclei from all the eight (T3+T2 sites) and six (T3 site only) histidine ligands are observed in SLAC-T1D and SLAC-wt respectively (Chapters 3 and 4). In the NI state five chemical exchange processes are identified and

## Chapter 7

are attributed to the histidine ligands ring motion at the TNC (Chapters 2 and 3). The exchange rates of these process suggest that they are independent processes. However, the energy barrier is similar within the one standard deviation (Chapter 2). The different rates suggest multiple reorganization events in the TNC and some of them might be a conformation that helps in progressing the oxygen reduction reaction to next step. These chemical exchange processes are not observed in the RO state. This may be due to the RO state being more rigid compared to the NI state thus slowing down the histidine ring motions to bring it outside the observed exchange rates of 80 to 200 s<sup>-1</sup>.

For further characterization of the chemical exchange processes, sequence specific assignment is needed. Using the second shell mutation of Y108F in SLAC-T1D, two of these processes were assigned to the T2 site histidine ligands (Chapter 3). A second shell mutation of Q291E in the SLAC-T1D resulted in the NMR spectra exclusively for the RO state. This is in contrast to the SLAC-T1D/Y108F mutant that was a mix of the NI and the RO state, with the former being the dominant species, analogous to the SLAC-T1D. The switch to the RO state allowed resonance assignment of two T3 site histidine ligands from the RO state. In addition, it revealed the subtle balance between the NI and the RO state. Perhaps this can be explained as follows. Gln291 is located near the T3 site, lining the water channel. This water channel was hypothesized to be the source of protons during the oxygen reduction. The NI state can be converted to the RO state by addition of two protons (Figure 1.3), which are obtained from the environment. Gln291 might well be one of the residues responsible for providing the protons, provided it simultaneously receives one from the surroundings. From the crystal structure 3cg8 of SLAC from *S. coelicolor*, the side chain of Gln291 is strongly hydrogen bonded to Thr167 O<sub>γ1</sub>, His164 CO and two water molecules (614 and 732) (Figure 7.1a).<sup>(18)</sup> Mutating it to Glu291 increases the proton donating ability and thus the NI state can be converted to the RO state for the SLAC-T1D/Q291E mutant with ease. In experiments not reported in the chapters before, we observed a time and pH dependent formation of an unknown state X from SLAC-T1D (Figure 7.1b, c and d). The protein was purified at pH 6.8 and after buffer exchange to pH 8.1 or 7.5 state X is populated in ~ 100 hrs. This state X can be reversed to the initial state, which is a mix of the RO and the NI state with latter being the dominant species, when the pH is lowered again to 6.8. The rate of formation of state X is slower at pH 7.5 than at pH 8.1. In state X the resonances of the NI state (22 to 55 ppm) are reduced in intensity, while those of the RO state (11 to 22 ppm) increase (Figure 7.1b and d). Two additional resonances, pa and pb, are observed in state X (Figure 7.1b and d). Perhaps this state is an intermediate between the NI and the RO states and is accessible at pH > 7.0 because a basic pH can locally increase the proton chemical potential. The pH dependence shown in Figure 7.1b, c and d might well be related to Gln291 donating a single proton and populating a state X that can be a partially

protonated NI state. The existence of such state was reported in Fet3p, an iron oxidizing laccase from *S. cerevisiae* (Figure 7.2).<sup>(19)</sup> Determining the pH dependence of the spectrum of SLAC-T1D/Q291E might give more insight into the role of the Gln291 residue in the oxygen reduction reaction and explain the reason of its slow rate of conversion. EPR spectroscopy in combination with quantum calculations might help to resolve the nature of state X and establish the role of Gln291.

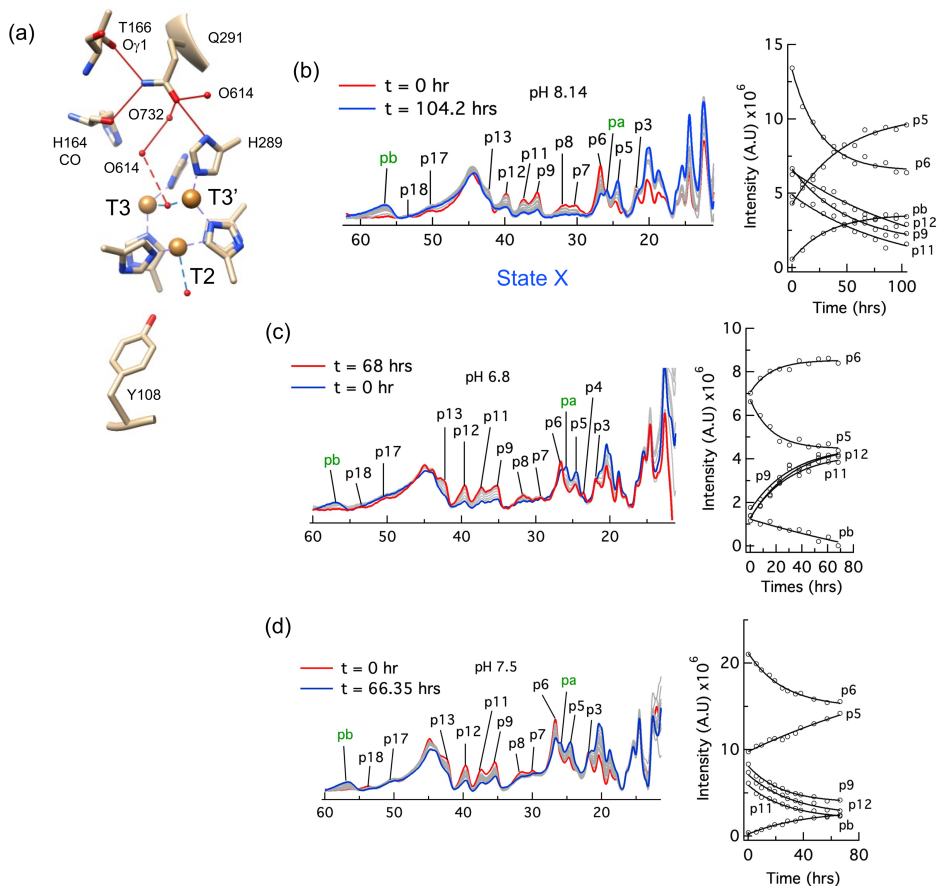


**Figure 7.1.** (a) The hydrogen bonding network of the Gln291 side chain. Orange spheres are the copper ions of the TNC. Respective copper ions are indicated. Amino acid residues are shown as wheat sticks. Red spheres are bound water molecules. Residues involved in the hydrogen bond (red sticks) are indicated. A probable hydrogen bond between O614 and the T3 copper ions bridging O is shown as dashed line. The time course <sup>1</sup>H NMR spectra of SLAC-T1D at pH 8.14 (b), 6.8 (c) and 7.5 (d). Panel b and c are sequential experiments while panel d is an independent sample. The time course is color coded as red (initial in panel b and d and final in panel c) and blue (final in panel b and d and initial in panel c). The blue trace is of state X as indicated below panel b. Intermediate time spectra are shown as grey

trace. Each panel is associated with the intensity change of the resonances with time. The solid line shows the single exponential fit of the data points in open circles.

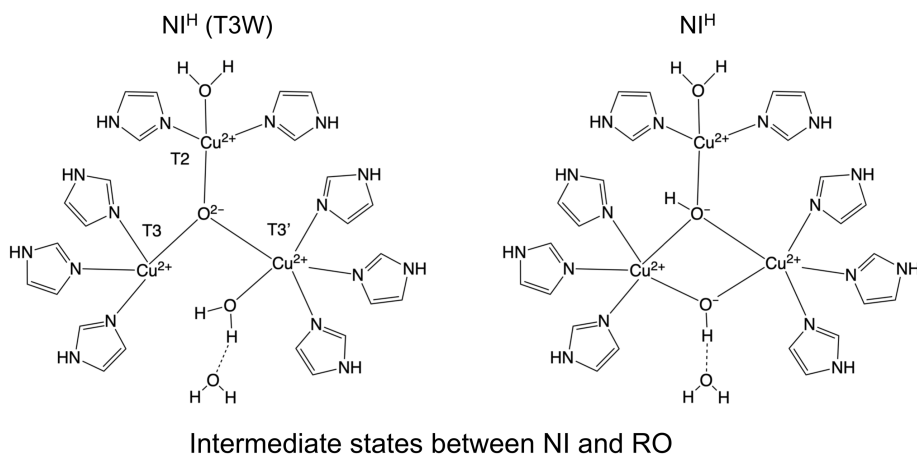


**Figure 7.2.** Proposed intermediate states during the conversion of the NI state to the RO state as described by Heppner et al. (2014).(19)

### Suggestions to obtain further assignments.

Overall, 2/8 histidine ligands in the NI state, one chemical exchange process and 2/6 histidine ligands from the RO state could be assigned sequence specifically. Maybe more second shell mutation can help in assigning resonances to other histidine ligands. Multiple amino acids can be subjected to mutagenesis as shown in Figure 1.2d, for example D113N, I169V, H164A and S294A. All these residues have interactions with the coordinating histidine ligands. Another method that can aid in assignment is using quantum calculations.(20) Such calculations have been extensively done for three-domain laccase, which lacks the Tyr near the T2 site.(15, 21) For SLAC it was reported that this residue plays an important role during catalysis and confers protection against the reactive oxygen species.(22, 23) The calculations on the basic model of the TNC in the RO state with the Tyr revealed that the orientation of the phenolic group determines the formation of the tyrosyl radical (Chapter 5). Radical formation is observed when the phenolic group is oriented toward the water/OH<sup>-</sup> ligand of the T2 site. Perhaps the tyrosyl radical in the calculation is an excited state of the RO state that is accessible only when the TNC is partially reduced, as observed experimentally.(22, 23) Using previous calculations as a benchmark (24), optimized geometry of the RO state could be obtained (Chapter 5). A similar strategy can be used to obtain geometry of the other intermediate states. These optimized geometries can be used to estimate the chemical shift on the histidine ligands, thereby aiding in the assignment of the observed resonances.

In paramagnetic solution NMR the signals are affected by two relaxation processes, (i) the interaction between the electron and nuclear spins or the Solomon-Bloembergen dipolar and contact mechanism and (ii) the interaction of the nuclear spin with the net magnetic moment in thermal equilibrium due to the rapid electronic relaxation rate or the Curie mechanism.<sup>(25)</sup> The Curie relaxation depends on the size of the molecule with relaxation increasing with the size of the molecule. Solid-state NMR (ssNMR) is independent of the molecular size and to a first approximation the contribution from the Curie mechanism is diminished or absent.<sup>(25)</sup> This results in observation of resonances from the nuclei very close ( $\sim 3.0 \text{ \AA}$ ) to the paramagnetic metal center.<sup>(20)</sup> In addition, dipolar couplings can be measured with high accuracy using ssNMR and this can provide anisotropic motions associated with residues near the metal centers.<sup>(11, 26)</sup> Unfortunately, in our hands SLAC was not stable under MAS conditions and paramagnetic signals vanished within a few hours. In Chapter 6 the efficacy of REDOR and shifted-REDOR in determining dipolar coupling strength in a strongly paramagnetic environment is shown. Multidimensional ssNMR experiments based on the dipolar coupling were optimized for application to paramagnetic molecules. As a future outlook these experiments can be applied to study the active site of laccase in greater detail, provided SLAC can be stabilized for experiments under MAS conditions.

## References

1. Vincent, K.A., J.A. Cracknell, J.R. Clark, M. Ludwig, O. Lenz, B. Friedrich, and F.A. Armstrong. 2006. Electricity from low-level  $\text{H}_2$  in still air – an ultimate test for an oxygen tolerant hydrogenase. *Chem. Commun.* 5033.
2. Vincent, K.A., J.A. Cracknell, A. Parkin, and F.A. Armstrong. 2005. Hydrogen cycling by enzymes: electrocatalysis and implications for future energy technology. *Dalton Trans.* 3397.
3. Sony Develops. *Sony Global - Sony Global Headquarters*.
4. Thorseth, M.A., C.E. Tornow, E.C.M. Tse, and A.A. Gewirth. 2013. Cu complexes that catalyze the oxygen reduction reaction. *Coordination Chemistry Reviews*. 257:130–139.
5. Plapp, B.V. 2010. Conformational Changes and Catalysis by Alcohol Dehydrogenase. *Arch Biochem Biophys*. 493:3–12.
6. Poulos, T.L. 2003. Cytochrome P450 flexibility. *Proceedings of the National Academy of Sciences*. 100:13121–13122.
7. Hammes-Schiffer, S. 2002. Impact of Enzyme Motion on Activity. *Biochemistry*. 41:13335–13343.
8. Pell, A.J., G. Pintacuda, and C.P. Grey. 2019. Paramagnetic NMR in solution and the solid state. *Progress in Nuclear Magnetic Resonance Spectroscopy*. 111:1–271.
9. Bertini, I., S. Ciurli, A. Dikiy, R. Gasanov, C. Luchinat, G. Martini, and N. Safarov. 1999. High-Field NMR Studies of Oxidized Blue Copper Proteins: The Case of Spinach Plastocyanin. *Journal of the American Chemical Society*. 121:2037–2046.
10. Kervern, G., G. Pintacuda, Y. Zhang, E. Oldfield, C. Roukoss, E. Kuntz, E. Herdtweck, J.-M. Basset, S. Cadars, A. Lesage, C. Copéret, and L. Emsley. 2006. Solid-State NMR of a Paramagnetic DIAD-FeII Catalyst: Sensitivity, Resolution Enhancement, and Structure-Based Assignments. *J. Am. Chem. Soc.* 128:13545–13552.
11. Parthasarathy, S., Y. Nishiyama, and Y. Ishii. 2013. Sensitivity and Resolution Enhanced Solid-State NMR for Paramagnetic Systems and Biomolecules under Very Fast Magic Angle Spinning. *Acc. Chem. Res.* 46:2127–2135.

12. Ishii, Y., N.P. Wickramasinghe, and S. Chimon. 2003. A New Approach in 1D and 2D  $^{13}\text{C}$  High-Resolution Solid-State NMR Spectroscopy of Paramagnetic Organometallic Complexes by Very Fast Magic-Angle Spinning. *J. Am. Chem. Soc.* 125:3438–3439.
13. Kervern, G., G. Pintacuda, and L. Emsley. 2007. Fast adiabatic pulses for solid-state NMR of paramagnetic systems. *Chemical Physics Letters.* 435:157–162.
14. Machczynski, M.C., and J.T. Babicz. 2016. Correlating the structures and activities of the resting oxidized and native intermediate states of a small laccase by paramagnetic NMR. *Journal of Inorganic Biochemistry.* 159:62–69.
15. Solomon, E.I., A.J. Augustine, and J. Yoon. 2008.  $\text{O}_2$  Reduction to  $\text{H}_2\text{O}$  by the multicopper oxidases. *Dalton Trans.* 3921–3932.
16. Bertini, I., C. Luchinat, G. Parigi, and E. Ravera. 2017. NMR of paramagnetic molecules: applications to metalloproteins and models. Second edition. Amsterdam: Elsevier.
17. Kalverda, A.P., J. Salgado, C. Dennison, and G.W. Canters. 1996. Analysis of the paramagnetic copper(II) site of amicyanin by  $^1\text{H}$  NMR spectroscopy. *Biochemistry.* 35:3085–3092.
18. Skálová, T., J. Dohnálek, L.H. Østergaard, P.R. Østergaard, P. Kolenko, J. Dušková, A. Štěpánková, and J. Hašek. 2009. The Structure of the Small Laccase from *Streptomyces coelicolor* Reveals a Link between Laccases and Nitrite Reductases. *Journal of Molecular Biology.* 385:1165–1178.
19. Heppner, D.E., C.H. Kjaergaard, and E.I. Solomon. 2014. Mechanism of the Reduction of the Native Intermediate in the Multicopper Oxidases: Insights into Rapid Intramolecular Electron Transfer in Turnover. *J. Am. Chem. Soc.* 136:17788–17801.
20. Bertarello, A., L. Benda, K.J. Sanders, A.J. Pell, M.J. Knight, V. Pelmenschikov, L. Gonnelli, I.C. Felli, M. Kaupp, L. Emsley, R. Pierattelli, and G. Pintacuda. 2020. Picometer Resolution Structure of the Coordination Sphere in the Metal-Binding Site in a Metalloprotein by NMR. *J. Am. Chem. Soc.* 142:16757–16765.
21. Jones, S.M., and E.I. Solomon. 2015. Electron Transfer and Reaction Mechanism of Laccases. *Cell Mol Life Sci.* 72:869–883.
22. Tian, S., S.M. Jones, and E.I. Solomon. 2020. Role of a Tyrosine Radical in Human Ceruloplasmin Catalysis. *ACS Cent. Sci.*
23. Gupta, A., I. Nederlof, S. Sottini, A.W.J.W. Tepper, E.J.J. Groenen, E.A.J. Thomassen, and G.W. Canters. 2012. Involvement of Tyr108 in the Enzyme Mechanism of the Small Laccase from *Streptomyces coelicolor*. *Journal of the American Chemical Society.* 134:18213–18216.
24. Quintanar, L., J. Yoon, C.P. Aznar, A.E. Palmer, K.K. Andersson, R.D. Britt, and E.I. Solomon. 2005. Spectroscopic and Electronic Structure Studies of the Trinuclear Cu Cluster Active Site of the Multicopper Oxidase Laccase: Nature of Its Coordination Unsaturation. *J. Am. Chem. Soc.* 127:13832–13845.
25. Kervern, G., S. Steuernagel, F. Engelke, G. Pintacuda, and L. Emsley. 2007. Absence of Curie Relaxation in Paramagnetic Solids Yields Long  $^1\text{H}$  Coherence Lifetimes. *J. Am. Chem. Soc.* 129:14118–14119.
26. Schanda, P., and M. Ernst. 2016. Studying dynamics by magic-angle spinning solid-state NMR spectroscopy: Principles and applications to biomolecules. *Progress in Nuclear Magnetic Resonance Spectroscopy.* 96:1–46.

